

ARTICLE TYPE

The Sequential Test for Chaos

Marat Akhmet*¹ | Mehmet Onur Fen†² | Astrit Tola‡³¹Department of Mathematics, Middle East Technical University, Turkey²Department of Mathematics, TED University, Turkey³Department of Mathematics, Middle East Technical University Turkey

Correspondence

* Email: marat@metu.edu.tr

† Email: monur.fen@gmail.com

‡ Email: astrittola@gmail.com

Present Address

This is sample for present address text this is sample for present address text

Summary

This paper reveals a novel numerical method, the sequential test, which approves chaos through sequences of numbers observations. The method aligns alongside the Lyapunov exponent and bifurcation diagram test. Explicitly elucidation of the method application for both continuous and discrete systems was given affiliated with the corresponding algorithms. The theoretical results are exemplified on systems satisfying different types of definitions of chaos or numerical methods. The results are supplemented with illustrative graphics.

KEYWORDS:

Chaotic dynamics, Numerical analysis, Sequential Test, Convergence sequence, Separation sequence

1 | INTRODUCTION AND PRELIMINARIES

At the turn of the nineteenth century, H. Poincaré started to consider chaotic dynamics. Later on, E. Lorenz¹³, Y. Ueda²⁰, T. Li and J. A. Yorke¹² and many others significantly developed the theory of chaos.

One can indicate chaos presence either *verifying through a definition* or by *numerical observations*. In the first case, one should consider ingredients of chaos for Devaney's⁹, Li-Yorke's¹², and Poincaré's⁵ chaos definitions, and to observe chaos numerically scientists use bifurcation diagrams or Lyapunov exponents^{2,16}. Usually numerical observations of chaos does not confirm which type of chaos is satisfied, but in our research, we suggest a novel approach which may approve definition Poincaré chaos through number sequences observations, that is through *the sequential test*. That is, we give arguments numerically and show that they are for the chaos.

Evaluating the Lyapunov exponent numerical method (LEM) is employed much widely to indicate chaos since it is universally applicable. Nevertheless, the idea is not accepted as a rigorous one since there are examples of nonchaotic systems with positive Lyapunov exponents². In contrast, the bifurcation diagram analysis method confirms chaos within systems possessing periodic solutions. Our numerical method, the sequential test, is applied to every system which possesses Poisson stable trajectory. Since this method theoretically will request infinitely many iterations to indicate chaos, the same as other methods, we will apply it and embrace the result for a finite number of iterations.

Let us denote \mathbb{N} the set of non-negative integers, and consider a metric (X, d) and a map $\pi : \mathbb{T}_+ \times X \rightarrow X$, where \mathbb{T}_+ is either the set of non-negative real numbers or \mathbb{N} , be a semi-flow on X , i.e., $\pi(0, x) = x$ for all $x \in X$, $\pi(t, x)$ is continuous in the pair of variables t and x , and $\pi(t_1, \pi(t_2, x)) = \pi(t_1 + t_2, x)$ for all $t_1, t_2 \in \mathbb{T}_+$, $x \in X$.

A point $x \in X$ is called positively Poisson stable (stable P^+)¹⁹ if there exists a sequence $\{t_n\}$ satisfying $t_n \rightarrow \infty$ such that $\pi(t_n, x) \rightarrow x$, as $n \rightarrow \infty$. For a given point $x \in X$, let Θ_x be the closure of the trajectory $T(x) = \{\pi(t, x) : t \in \mathbb{T}_+\}$. The set Θ_x is a quasi-minimal set if the point x is stable P^+ and $T(x)$ is contained in a compact subset of X ¹⁹.

In paper⁶ the definitions of an unpredictable point and Poincaré chaos was introduced.

Definition 1. ⁽⁶⁾. A point $p \in X$ and the trajectory through it are unpredictable if there exist a positive number ε_0 (the unpredictability constant) and sequences $\{t_n\}$ and $\{s_n\}$, both of which diverge to infinity, such that $f(t_n, p) \rightarrow p$ as $n \rightarrow \infty$ and $d[f(t_n + s_n, p), f(s_n, p)] > \varepsilon_0$ for each $n \in \mathbb{N}$.

One can see that if a point is unpredictable then it is Poisson stable.

The paper⁶ reveals the presence of sensitivity and transitivity in a set Θ_p if p is an unpredictable point in X . Their presence in a quasi-minimal set Θ_p within p being an unpredictable point, exposed the appearance of chaos, which was a new chaos type named after Poincaré. Thus the following definition was accepted.

Definition 2. ⁽⁶⁾. The dynamics on the quasi-minimal set Θ_p is called Poincaré chaotic if p is an unpredictable point.

In paper⁶, the following Theorem 1 was proven.

Theorem 1. ⁽⁶⁾. Suppose that $p \in X$ is stable P^+ and $T(p)$ is contained in a compact subset of X . If Θ_p is neither a rest point nor a cycle, then it contains an uncountable set of motions everywhere dense and stable P^+ .

It is worth noting that in the paper⁶, it was proved that if p is an unpredictable point, then the dynamics on p is sensitive. That is, there exists a positive number $\tilde{\varepsilon}_0$ such that for each $x_1 \in \Theta_p$ and for each positive number δ there exist a point $x_2 \in \Theta_p$ and a positive number \tilde{t} such that $d(x_1, x_2) < \delta$ and $d(f(\tilde{t}, x_1), f(\tilde{t}, x_2)) \geq \tilde{\varepsilon}_0$.

In paper⁷, the definition of unpredictable functions was introduced and it was adapted to the theory of differential equations. In other words, unpredictable functions are considered the solutions of differential equations.

Definition 3. ⁽⁷⁾. A uniformly continuous and bounded function $\vartheta : \mathbb{R} \rightarrow \mathbb{R}^m$ is unpredictable if there exist positive numbers ε_0, δ and sequences $\{t_n\}, \{s_n\}$ both of which diverge to infinity such that $\|\vartheta(t + t_n) - \vartheta(t)\| \rightarrow 0$ as $n \rightarrow \infty$ uniformly on compact subsets of \mathbb{R} and $\|\vartheta(t + t_n) - \vartheta(t)\| \geq \varepsilon_0$ for each $t \in [s_n - \delta, s_n + \delta]$ and $n \in \mathbb{N}$.

Since to create Poincaré chaos⁶ uniform continuity is not a necessary condition for an unpredictable function ϑ , in paper⁷ the Definition 3 was adjusted as follows.

Definition 4. ⁽⁷⁾. A continuous and bounded function $\vartheta : \mathbb{R} \rightarrow \mathbb{R}^m$ is unpredictable if there exist a positive number ε_0 and sequences $\{t_n\}, \{s_n\}$ both of which diverge to infinity such that $\|\vartheta(t + t_n) - \vartheta(t)\| \rightarrow 0$ as $n \rightarrow \infty$ uniformly on compact subsets of \mathbb{R} and $\|\vartheta(t_n + s_n) - \vartheta(s_n)\| \geq \varepsilon_0$ for each $n \in \mathbb{N}$.

For the convenience of the next discussion, we will call the convergence of the function's shifts on compact subsets and the existence of the sequence $\{t_n\}$ as *Poisson stability of the unpredictable function* or simply Poisson stability, and the existence of the number ε_0 and the sequence $\{s_n\}$ as *unpredictability property* of the function. Thus, a function is unpredictable, if it is *Poisson stable* and admits the *unpredictability property*.

The next, Definition 5 and Definition 6, are the instruments for the numerical analysis in this paper.

Definition 5. ⁽⁷⁾. A continuous and bounded function $\vartheta : \mathbb{R} \rightarrow \mathbb{R}^m$ is unpredictable if there exist a positive number ε_0 and sequences $\{t_n\}, \{s_n\}$ both of which diverge to infinity such that $\|\vartheta(t_n) - \vartheta(0)\| \rightarrow 0$ as $n \rightarrow \infty$ and $\|\vartheta(t_n + s_n) - \vartheta(s_n)\| \geq \varepsilon_0$ for each $n \in \mathbb{N}$.

In⁷ was also given the definition of the unpredictable sequence. Here, unpredictable sequences are considered as the solutions of discrete equations.

Definition 6. ⁽⁷⁾. A bounded sequence $\kappa_i, i \in \mathbb{N}$, in \mathbb{R}^p is called unpredictable if there exist a positive number ε_0 and sequences $\{\zeta_n\}, \{\eta_n\}, n \in \mathbb{N}$, of positive integers both of which diverge to infinity such that $\|\kappa_{\zeta_n} - \kappa_0\| \rightarrow 0$ as $n \rightarrow \infty$ and $\|\kappa_{\zeta_n + \eta_n} - \kappa_{\eta_n}\| \geq \varepsilon_0$ for each $n \in \mathbb{N}$.

In course of this definitions, we will suggest the sequential test. Consider the autonomous system of differential equations

$$x'(t) = f(x(t)), \quad (1)$$

where $f : \mathbb{R}^m \rightarrow \mathbb{R}^m$ is a continuous function. Let $x(t)$ be the solution of system (1) with initial condition $x(0) = x_0$, where x_0 is a given point in \mathbb{R}^m .

According to Definition 5, we say that the solution $x(t)$ satisfies the *sequential test*, if it is confirmed numerically that there exist a large natural number k and a positive number ε_0 , sequences $\{t_n\}$ and $\{s_n\}$, where $1 \leq n \leq k$, for the solution, such that $\|x(t_n) - x(0)\| = \delta_n$ is a decreasing sequence which becomes close to 0 and the inequality $\|x(t_n + s_n) - x(s_n)\| > \varepsilon_0$ is valid for

every $1 \leq n \leq k$. The largest value of t_k may reach $1.9 \cdot 10^6$, as well as the smallest δ_k are of order 10^{-3} . For continuous systems. For discrete models the largest values ζ_k are of order 10^8 and α_k are small, of order 10^{-6} . The value of number k , as well as the smallness of δ_n , are closely related to the power and facilities offered by a computer, and length of time interval. It is obvious that in different calculations with different ε_0 , δ_n or computers, similar results are not obtained. So the sequences $\{t_n\}$ and $\{s_n\}$ are not unique for a given solution. For convinience, we will call $\{t_n\}$ *the sequence of convergence* and $\{s_n\}$ *the sequence of separation*. In the light of Definition 5, one may say that the solution is unpredictable and the system (1) is Poincaré chaotic if the sequential test is satisfied.

It is our hypothesis that if the sequential test works for a sufficient large interval of time, then the Poincaré chaos is present. In other words, if the test is confirmed for any interval of time preserving the conditions of the test. We suppose that the theorem of this kind can be proved and suggest the assertion as an open problem. The proof of theorem may follow the arguments for Shadowing theorem^{8,6,14,17,10,15}.

In order that, system (1) satisfies the sequential test, we numerically evaluated the sequence $\{t_n\}$ on time interval $(t_{fix}, t_{final}]$, where t_{final} is a large real positive number and $0 \leq t_{fix} < t_{final}$ is a fixed number. Since δ_n is a decreasing sequence which becomes close to 0 then the inequality $\delta_n < \frac{1}{n}$ is valid for some n , where $1 \leq n \leq k$. We used this inequality for all systems considered in this paper, on which sequential test is applied. In order to obtain increasing sequences, $\{t_n\}$ and $\{s_n\}$, we set the condition

$$(CI) \quad t_{\xi+1} > t_{\xi} \text{ and } s_{\xi+1} > s_{\xi}, \xi = 1, 2, 3, \dots$$

Succeeding, we will provide some description of the detailed steps which will be applied later to construct Matlab codes as Algorithm 1.

Let $n = 1$ and $\tau_m = mh$, $m = 1, 2, \dots$

While $\|x(\tau_m) - x(0)\| < \frac{1}{1}$,

fix $t_1 = \tau_{m_1}$ the first value of τ_m 's satisfying the inequalities $\|x(\tau_m) - x(0)\| < 1$ and $\tau_{m_1} > t_{fix}$.

Set $\tau_i^* = ih$, $i = 1, 2, \dots$

While $\|x(t_1 + \tau_i^*) - x(\tau_i^*)\| > \varepsilon_0$,

fix $s_1 = \tau_{i_1}^*$ the first value of τ_i^* 's satisfying the inequality $\|x(t_1 + \tau_i^*) - x(\tau_i^*)\| > \varepsilon_0$.

Let $n = 2$.

While $\|x(\tau_m) - x(0)\| < \frac{1}{2}$,

fix $t_2 = \tau_{m_2}$ the first value of τ_m 's satisfying the inequalities $\|x(\tau_m) - x(0)\| < \frac{1}{2}$ and $\tau_{m_2} > t_1$.

While $\|x(t_2 + \tau_i^*) - x(\tau_i^*)\| > \varepsilon_0$,

fix $s_2 = \tau_{i_2}^*$ the first value of τ_i^* 's satisfying the inequalities $\|x(t_2 + \tau_i^*) - x(\tau_i^*)\| > \varepsilon_0$ and $\tau_{i_2}^* > s_1$

Let $n = N$, where $1 \leq N \leq k$.

While $\|x(\tau_m) - x(0)\| < \frac{1}{N}$,

fix $t_N = \tau_{m_N}$ the first value of τ_m 's satisfying the inequalities $\|x(\tau_m) - x(0)\| < \frac{1}{N}$ and $\tau_{m_N} > t_{N-1}$.

While $\|x(t_N + \tau_i^*) - x(\tau_i^*)\| > \varepsilon_0$,

fix $s_N = \tau_{i_N}^*$ the first value of τ_i^* 's satisfying the inequalities $\|x(t_N + \tau_i^*) - x(\tau_i^*)\| > \varepsilon_0$ and $\tau_{i_N}^* > s_{N-1}$.

In what follows, the Matlab code based on the above description will be as follows.

Algorithm 1 Sequential test for system (1)

```

1: Input  $t_{fix}$ 
2: Set  $l = t_{fix}$ 
3: Set  $q = 0$ 
4: Input  $\varepsilon_0$ 
5: Input  $nspart$  ▷ number of iterations
6: Set  $tmin = 0$ 
7: Set  $dt = 0.01$ 
8: Find  $tmax = nspart \cdot dt$ 
9: Input initial condition  $x_0$ 
10: Find the numerical solution  $x(t)$  of system 1 for the given interval.
11: for  $n = 1 : k$  do
12:   for  $m = 1 : nspart$  do
13:     if  $\|x(\tau_m) - x(0)\| < \frac{1}{n}$  then
14:       if  $l < \tau_m$  then
15:          $l = \tau_m$ 
16:          $A(n) = l$  ▷ the matrix  $A(n)$  collects  $\tau_m$ 's, which satisfy lines 13 and 14 for each  $n$ 
17:         break ▷ reckon the first  $\tau_m$  replenishing lines 13 and 14 for each  $n$ 
18:       end if
19:     end if
20:   end for
21: end for
22: for  $n = 1 : k$  do
23:   for  $i = 1 : nspart$  do
24:     if  $\|x(A(n) + \tau_i^*) - x(\tau_i^*)\| > \varepsilon_0$  then
25:       if  $q < \tau_i^*$  then
26:          $q = \tau_i^*$ 
27:          $B(n) = q$  ▷ the matrix  $B(n)$  collects  $\tau_i^*$ 's, which satisfy lines 24 and 25 for each  $n$ 
28:         Display matrices  $A(n)$  and  $B(n)$ 
29:         break ▷ reckon the first  $\tau_i^*$  replenishing lines 24 and 25 for each  $n$ 
30:       end if
31:     end if
32:   end for
33: end for

```

The sequential test is also applicable on solutions of discrete systems. For this purpose, consider the autonomous discrete system

$$x(i+1) = f(x(i)), \quad (2)$$

where $f : \mathbb{R} \rightarrow \mathbb{R}^m$ is a continuous function. Let $x(i) = x_i$ be the solution of system (2) with initial condition $x(0) = x_0$, where x_0 is a given point in \mathbb{R}^m .

According to Definition 6, we say that the solution x_i satisfies the *sequential test*, if it is confirmed numerically that there exist a large natural number k and a positive number ε_0 , increasing sequences of natural numbers $\{\zeta_n\}$ and $\{\eta_n\}$, where $1 \leq n \leq k$, for the solution, such that $\|x_{\zeta_n} - x_0\| = \alpha_n$ is a decreasing sequence which approaches to 0 and the inequality $\|x_{\zeta_n + \eta_n} - x_{\eta_n}\| > \varepsilon_0$ is valid for every $1 \leq n \leq k$. Similarly, as in the case of autonomous systems of differential equations, the sequences $\{\zeta_n\}$ and $\{\eta_n\}$ are not unique for a given solution. For convenience, we will call $\{\zeta_n\}$ *the sequence of convergence* and $\{\eta_n\}$ *the sequence of separation*. Setting side by side with Definition 6, one may say that the solution is unpredictable and the system (2) is Poincaré chaotic if the sequential test is satisfied.

Carrying on, we will present how to create a MATLAB function for the sequential test for autonomous discrete systems. For this reason, consider system (2) with its solution x_i and initial condition x_0 , where the solution x_i satisfies the sequential test for a positive value ε_0 . Based on the following rationalizing, we will erect the upcoming Algorithm 2.

In order that, system (2) replenishes the sequential test we numerically evaluated the sequence $\{\zeta_n\}$ on interval $(i_{fix}, i_{final}]$, where i_{final} is a large natural number and $0 \leq i_{fix} < i_{final}$ is a fixed number. Since α_n is a decreasing sequence which becomes close to 0 then the inequality $\alpha_n < \frac{1}{n}$ is valid for some n , where $1 \leq n \leq k$. We adopted this inequality for all discrete systems analyzed in this paper, on which sequential test is implemented. In order to obtain increasing sequences, $\{\zeta_n\}$ and $\{\eta_n\}$, we set the condition

$$(C2) \quad \zeta_{\xi+1} > \zeta_k \text{ and } \eta_{\xi+1} > \eta_k, \xi = 1, 2, 3, \dots$$

Following, we will implement some explanation of the detailed steps which will be used later to construct Matlab codes as Algorithm 2.

Let $n = 1$ and $m = 1, 2, \dots$

While $\|x_m - x_0\| < \frac{1}{1}$,

fix $\zeta_1 = m_1$ the first value of m 's satisfying the inequalities $\|x_m - x_0\| < 1$ and $m_1 > i_{fix}$.

Set $m^* = 1, 2, \dots$

While $\|x_{\zeta_1+m^*} - x_{m^*}\| > \varepsilon_0$,

fix $\eta_1 = m_1^*$ the first value of m^* 's satisfying the inequality $\|x_{\zeta_1+m^*} - x_{m^*}\| > \varepsilon_0$.

Let $n = 2$.

While $\|x_m - x_0\| < \frac{1}{2}$,

fix $\zeta_2 = m_2$ the first value of m 's satisfying the inequalities $\|x_m - x_0\| < 1$ and $m_2 > m_1$.

While $\|x_{\zeta_2+m^*} - x_{m^*}\| > \varepsilon_0$,

fix $\eta_2 = m_2^*$ the first value of m^* 's satisfying the inequality $\|x_{\zeta_2+m^*} - x_{m^*}\| > \varepsilon_0$ and $m_2^* > m_1^*$.

Let $n = N$, where $1 \leq N \leq k$.

While $\|x_m - x_0\| < \frac{1}{N}$,

fix $\zeta_N = m_N$ the first value of m 's satisfying the inequalities $\|x_m - x_0\| < 1$ and $m_N > m_{N-1}$.

While $\|x_{\zeta_N+m^*} - x_{m^*}\| > \varepsilon_0$,

fix $\eta_N = m_N^*$ the first value of m^* 's satisfying the inequality $\|x_{\zeta_N+m^*} - x_{m^*}\| > \varepsilon_0$ and $m_N^* > m_{N-1}^*$.

In what follows, the Matlab code based on the earlier explanation will be as follows.

Algorithm 2 Sequential test for system (2)

```

1: Input  $i_{fix}$ 
2: Set  $l = i_{fix}$ 
3: Set  $q = 0$ 
4: Input  $\varepsilon_0$ 
5: Input  $nspart$  (number of iterations)
6: Input initial condition  $x_0$ .
7: Find the numerical solution  $x_i$  of system 2 for the given interval
8: for  $n = 1 : k$  do
9:   for  $m = 1 : nspart$  do
10:    if  $\|x_m - x_0\| < \frac{1}{n}$  then
11:      if  $l < m$  then
12:         $l = m$ 
13:         $A(n)=l$  ▷ the matrix A(n) collects  $m$ 's, which satisfy lines 10 and 11 for every n
14:        break ▷ reckon the first  $m$  replenishing lines 10 and 11 for each n
15:      end if
16:    end if
17:  end for
18: end for
19: for  $n = 1 : k$  do
20:   for  $m^* = 1 : nspart$  do
21:    if  $\|x_{A(n)+m^*} - x_{m^*}\| > \varepsilon_0$  then
22:      if  $q < m^*$  then
23:         $q=m^*$ 
24:         $B(n)=q$  ▷ the matrix B(n) collects  $m^*$ 's, which satisfy lines 21 and 22 for every n
25:        Display matrices  $A(n)$  and  $B(n)$ 
26:        break ▷ reckon the first  $m^*$  replenishing lines 21 and 22 for each n
27:      end if
28:    end if
29:  end for
30: end for

```

In this paper, we will apply the Algorithm 1 or Algorithm 2 to construct the sequences of convergence, $\{t_n\}$ or $\{\zeta_n\}$, and the sequence of divergence $\{s_n\}$ or $\{\eta_n\}$, respectively, for concrete models that satisfy the sequential test. In other words, the algorithms are the basis of the test.

2 | DEVANEY'S CHAOS SUBDUED TO THE SEQUENTIAL TEST

One of the definitions of chaos was provided by Devaney⁹ in 1976. To present this definition let us consider the autonomous discrete system

$$x_{i+1} = G(x_i), \quad (3)$$

where $G : J \rightarrow J$, J is the solution space, be continuous. A point $p \in J$ is a **periodic point** if $G^n(p) = p$, for some $n \geq 1$, and $G^k(p) \neq p$, for $1 \leq k < n$. $G : J \rightarrow J$ is said to be **topologically transitive** if there is a point $x_0 \in J$ such that the orbit of x_0 is dense in J . $G : J \rightarrow J$ is said to have **sensitive dependence** on initial conditions if there exists $\delta > 0$ such that, for any $x \in J$ and every $\varepsilon > 0$, there exists $y \in J$ and $n \geq 0$ such that $|x - y| < \varepsilon$, $|G^n(x) - G^n(y)| > \delta$.

Definition 7. ⁽⁹⁾. The function G is said to be chaotic if:

- i. G has sensitive dependence on initial conditions.
- ii. G is topologically transitive.
- iii. periodic points are dense in J .

One of the most known Devaney chaotic equation is Hénon map. It was introduced on 1975 by the french astronomer M. Hénon². Also you can see in² that this map has positive Lyapunov exponents. In his book⁹ Devaney proved that Hénon map was Devaney chaotic. Now we will analyse if it is Poincaré chaotic by using the sequential test. Let us consider the following map:

$$\begin{aligned} x_{n+1} &= 1 - 1.4x_n^2 + y_n \\ y_{n+1} &= 0.3x_n. \end{aligned} \quad (4)$$

For this system we took the initial values $[-0.27518575309954679, -0.32515652033839654]$. Figure 1 (a) shows the trajectory of system (4) within the initial values and Figure 1 (b) represents the solution graphs of each coordinate with respect to index i .

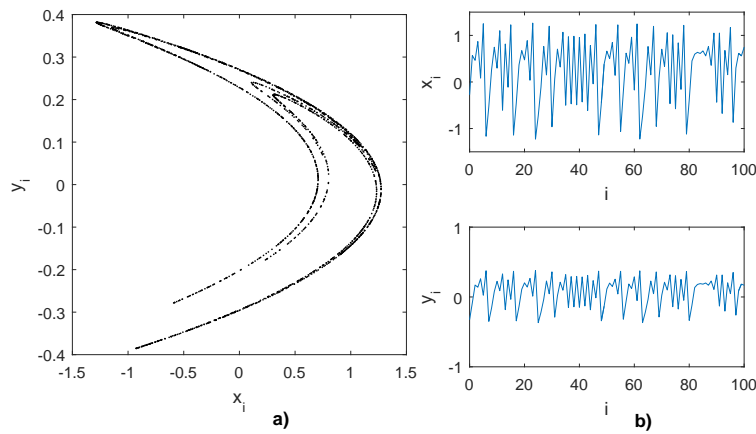


FIGURE 1 Simulations for the solution of system (4) with the given initial values: **(a)** the trajectory of the solution, **(b)** the solution graphs of each coordinate with respect to index i .

We will implement the Sequential Test through Algorithm 2 to system (4) with the fixed initial conditions and $\varepsilon_0 = 2.1$. The index i starts at 0 and prolongs till 10^8 . As a result, we obtained 4219 terms for each sequence and selected 11 of them are shown in Table 1 .

n	k	1/k	ζ_k	η_k
1	1	1	2	180
2	2	0.5	7	181
3	619	0.001616	1527239	15364
4	1084	0.000923	6504212	26361
5	1904	0.000525	28566825	48105
6	2337	0.000428	46003272	58728
7	2708	0.000369	65836673	68727
8	3008	0.000332	12056560	75921
9	3436	0.000291	113770045	86963
10	3710	0.00027	139217264	93357
11	4219	0.000237	199876783	105711

TABLE 1 Selected elements from the sequence of convergence and the sequence of separation obtained by Algorithm 2 applied on system (4).

Next, the results achieved by Algorithm 2 can be displayed graphically. For each element, say ζ_γ , within the sequence of convergence $\{\zeta_n\}$, can be drawn a particular graph of solutions of system (2) with initial conditions x_0 and $x(\zeta_\gamma)$. We will denote $x_{shift}(i) = x(i + \zeta_\gamma)$ the solution of the system within $x_0 = x(\zeta_\gamma)$. In these graphs will be visible the closeness at 0, and the separation bigger than ε_0 between the two solution curves at the corresponding element of the sequence of separation $\{\eta_n\}$, η_γ . We will use this representation on any result obtained by employing Algorithm 2.

Following, we will represent an individual graph associated with $\zeta_\gamma = \zeta_2 = 7$. Since it is difficult to analyze the two dimensional graph, we will show the graph of system (4) for one dimension, the one where the distance between $\omega_i = \omega(i)$ and $\omega_{shift}(i)$, $\omega = x, y$, is bigger than the other dimension at point $i = \eta_\gamma = \eta_2 = 181$. The distance at $\eta_2 = 181$ is bigger in x dimension. In Figure 2, the blue curve shows the graph of solution of (4), $x_i = x(i)$, where the initial condition is $X_0 = X(0)$, while the red curve is the solution where the initial value is $X_0 = X(7)$, $x_{shift}(i) = x(i + 7)$, where $X(i) = (x(i), y(i))$ and $X_{shift}(i) = (x_{shift}(i), y_{shift}(i))$. The green line segment connects the points $(181, x(181))$ and $(181, x_{shift}(181))$.

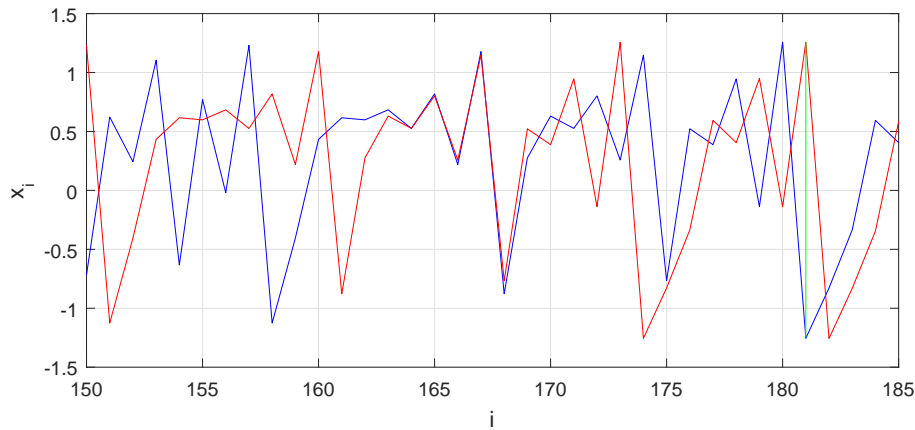


FIGURE 2 The blue curve shows the graph of solution of system (4), $x(i)$, while the red curve is $x_{shift}(i)$. The green line segment connects the points $(181, x(181))$ and $(181, x_{shift}(181))$ and presents the distance between the solutions at index $i = 181$.

The length of the green line segment is $|x(181) - x_{shift}(181)| = 2.5126048968 > \varepsilon_0$. In our calculation, we noticed that the distances,

$$|x(16) - x_{shift}(16)| = 2.4056956028,$$

$$|x(23) - x_{shift}(23)| = 2.2273052694,$$

$$|x(47) - x_{shift}(47)| = 2.3644760759,$$

$$|x(61) - x_{shift}(61)| = 2.2005894834,$$

$$|x(119) - x_{shift}(119)| = 2.267728785,$$

$$|x(126) - x_{shift}(126)| = 2.1601388248,$$

$$|x(174) - x_{shift}(174)| = 2.4024198634,$$

are bigger than ε_0 , while the index values are smaller than η_2 . Except for these indexes, this is also evident that two-dimensional distances $\|X(40) - X_{shift}(40)\| = 2.157836143$ and $\|X(72) - X_{shift}(72)\| = 2.1929991986$. The 2-dimensional distance between the two solution curves at $i = 181$ is $\|X(181) - X_{shift}(181)\| = 2.5472810502$. Succeeding, let us consider the closeness of solutions $X(i)$ and $X_{shift}(i)$ of system (4) on the interval $[340, 420]$. Figure 3 presents the graph of solutions $y(i)$ and $y_{shift}(i)$ on $[340, 420]$, where the solution curves are nigh.

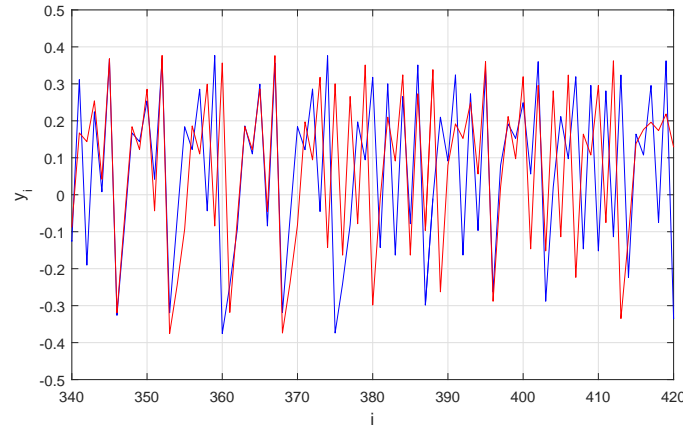


FIGURE 3 The blue and red curve present the solution of $y(i)$ and $y_{shift}(i)$ of system (4) on the interval $[340, 420]$.

It is seen from Figure 3, that the solutions $y(i)$ and $y_{shift}(i)$ are close to each other on the closed intervals $[343, 353]$, $[361, 368]$, $[384, 386]$, $[395, 400]$ and $[414, 417]$. The greatest distance between the two solution curves on these intervals is 0.1088336401. If we consider the two-dimensional graph, the solutions $X(i)$ and $X_{shift}(i)$ are close on the closed intervals $[344, 349]$, $[362, 364]$, $[384, 385]$, $[393, 399]$ and $[414, 415]$. The greatest two-dimensional distance between the two solution curves on these intervals is 0.1069390621.

3 | TESTIFYING LI-YORKE CHAOS

Li-Yorke chaos was introduced on 1975 in paper¹². To present this definition let J be an interval and consider the autonomous discrete system

$$x_{i+1} = F(x_i), \quad (5)$$

where $F : J \rightarrow J$ is continuous.

Definition 8. (¹²). The function F is said to be chaotic in the sense of Li-Yorke if:

T1. for every $k = 1, 2, 3, \dots$, there is a periodic point in J having period k .

T2. there is an uncountable set $S \in J$ (containing nonperiodic points), which satisfies the following conditions:

A) For every $p, q \in S$ with $p \neq q$

$$\lim_{n \rightarrow \infty} \sup |F^n(p) - F^n(q)| > 0 \quad (6)$$

and

$$\lim_{n \rightarrow \infty} \sup |F^n(p) - F^n(q)| = 0. \quad (7)$$

B) For every $p \in S$ and periodic point $q \in J$,

$$\lim_{n \rightarrow \infty} \sup |F^n(p) - F^n(q)| > 0. \quad (8)$$

In their paper¹² they also proved that the equation:

$$x_{i+1} = 3.9x_i(1 - x_i) \quad (9)$$

with initial condition $x(0) = 0.5$ is Li-Yorke chaotic.

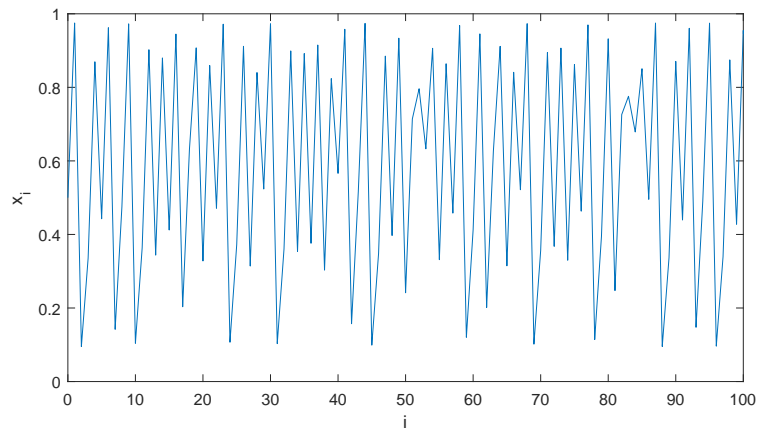


FIGURE 4 Solution of system (9) with the given initial condition.

We will apply the sequential test on this system within the set initial condition. The value i starts from 0 and prolongs till 10^8 . Let $\varepsilon_0 = 0.7$. For this system we obtained 17562 terms. In Table 2 are shown 11 selected elements from the sequence of convergence and the sequence of separation.

n	k	$1/k$	ζ_k	η_k
1	1	1	2	2
2	10	0.1	40	45
3	1905	0.000525	1190408	15836
4	3764	0.000266	4619782	30909
5	5251	0.000190	9081712	42939
6	6997	0.000143	16316573	57253
7	8298	0.000121	22776341	67995
8	9549	0.000105	29930023	78430
9	11026	0.000091	39821708	90551
10	12460	0.000080	50743495	10207
11	17562	0.000057	99977681	16027

TABLE 2 Selected elements from the sequence of convergence and the sequence of separation obtained from Algorithm 2 applied on system (9).

Succeeding, let us graph a particular graph associated with one element within the sequence of convergence presented in Table 2 . Let $\zeta_y = \zeta_{10} = 40$. The blue curve shows the graph of solution of (9) where the initial condition is $x_0 = x(0)$, while the red curve is the solution where the initial value is $x_0 = x(40)$. The green line segment connects the points $(45, x(45))$ and $(45, x_{shift}(45))$.

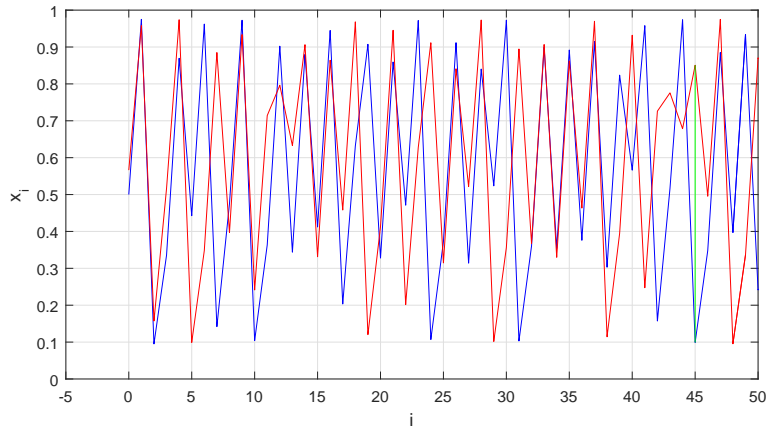


FIGURE 5 The blue curve shows the graph of solution of the system, $x(i)$, where the initial condition is $x_0 = x(0)$, while the red curve is the solution of system (9) with initial condition $x_0 = x(40)$, $x_{shift}(i)$. The green line segment connects the points $(45, x(45))$ and $(45, x_{shift}(45))$ and presents the distance between the solutions at index $i = 45$

The length of the green line segment is $|x(45) - x_{shift}(45)| = 0.7515802112 > \varepsilon_0$. In our calculations, we noticed that

$$|x(7) - x_{shift}(7)| = 0.7429614716,$$

$$|x(19) - x_{shift}(19)| = 0.7870394876,$$

$$|x(24) - x_{shift}(24)| = 0.8045231135,$$

$$|x(31) - x_{shift}(31)| = 0.7915891888,$$

$$|x(41) - x_{shift}(41)| = 0.7105760726,$$

where the index values are smaller than η_{10} . Next, let us consider the closeness of solutions $x(i)$ and $x_{shift}(i)$ of the system (9) on the interval $[30, 100]$. Figure 6 displays the graph of solutions on $[30, 100]$.

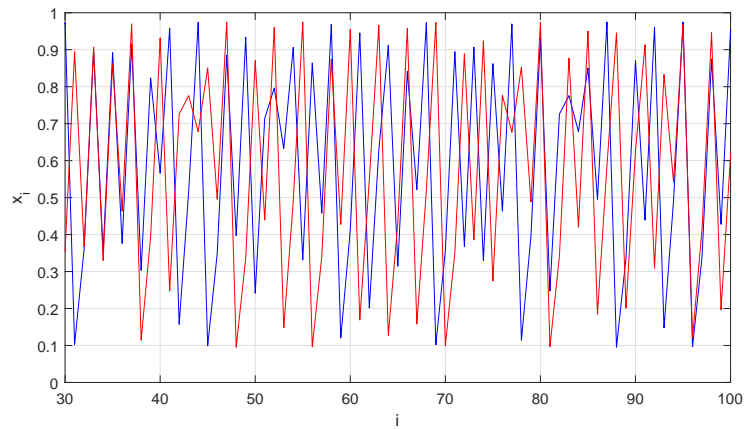


FIGURE 6 The blue and red curve present the solution of $x(i)$ and $x_{shift}(i)$ of system (9) on the interval $[30,100]$.

It is seen from Figure 6, that the solutions $x(i)$ and $x_{shift}(i)$ are close to each other on the closed intervals $[32,37]$, $[57,58]$, $[65,66]$, $[79,80]$ and $[94,98]$. The greatest distance between the two solution curves on these intervals is 0.1187907046.

4 | BIFURCATION DIAGRAM ANALYSIS (BDA) AND THE SEQUENTIAL TEST

BDA chaotic systems possess periodic solutions³. In⁴ one can find system (10) and that it is Period-Doubling Route chaotic

$$\begin{aligned} x_1' &= 10(x_2 - x_1) \\ x_2' &= 99.51x_1 - x_1x_3 - x_2 \\ x_3' &= x_1x_2 - \frac{8}{3}x_3. \end{aligned} \quad (10)$$

The initial conditions considered are $[23.319088231571342, -15.11725273004282, 130.76383915267931]$. Figure 7 (a) presents the trajectory of system (10) within initial conditions while Figure 7 (b) presents the solution graphs of each coordinate with respect to time t .

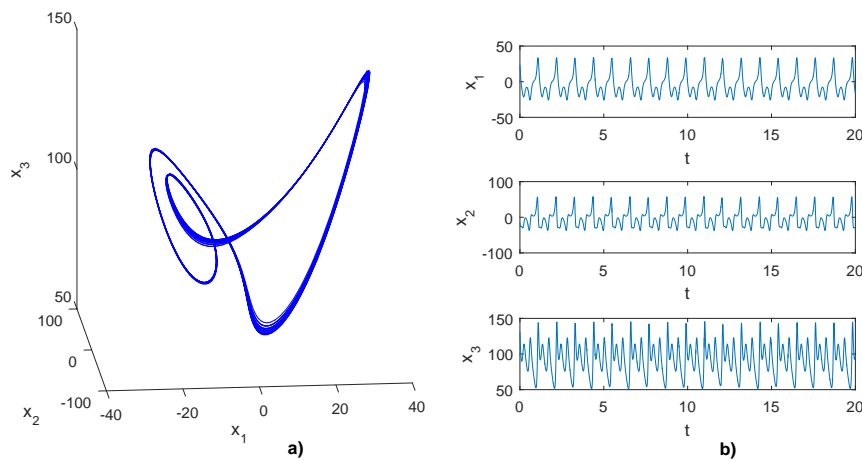


FIGURE 7 Simulations for the solution of system (10) with the given initial values: **(a)** the trajectory of the solution, **(b)** the solution graphs of each coordinate with respect to time t .

We will execute the sequential test through Algorithm 1 to system (10) with the fixed initial conditions. Time interval starts at 0 and prolongs till $1.3 \cdot 10^6$, partitioned into pieces with distance 0.01 and $\varepsilon_0 = 45$. In order that the system (10) satisfy the sequential test for $\varepsilon_0 = 45$, we skipped $t_{fix} = 631.36$ while evaluating the sequence of convergence $\{t_n\}$. Within the given conditions and time interval, we found that $k = 347$. In Table 3, are shown 10 selected elements from the sequence of convergence and the sequence of separation.

n	k	$1/k$	t_k	s_k
1	1	1	640.35	117.87
2	38	0.012195	13076.12	137.74
3	79	0.006711	68393.97	160.89
4	111	0.003937	118970.29	180.69
5	146	0.003311	234621.96	200.54
6	175	0.002519	280456.75	217.08
7	207	0.002079	331033.07	233.63
8	258	0.001706	592366.1	263.38
9	310	0.001464	846071.02	293.15
10	347	0.001186	1025217.53	313

TABLE 3 Selected elements from the sequence of convergence and the sequence of separation obtained from Algorithm 1 applied on system (10).

Succeeding, the results achieved by Algorithm 1 can be displayed graphically. For each element, say t_γ , within the sequence of convergence $\{t_n\}$, can be drawn a particular graph of solutions of the system (1) with initial conditions x_0 and $x(t_\gamma)$. We will denote $x_{shift}(t) = x(t + t_\gamma)$ the solution of the system within $x_0 = x(t_\gamma)$. In these graphs will be visible the closeness at 0, and the separation bigger than ε_0 between the two solution curves at the corresponding element of the sequence of separation $\{s_n\}$, s_γ . We will use this representation on any result obtained by employing Algorithm 1.

Following this description, we will draw a particular graph using $t_\gamma = t_1 = 640.35$. Since it is difficult to analyze the three dimensional graph, we will show the graph of solution for system (10) for one dimension with respect to time, the one where the distance between $x_\omega(t)$ and $x_{\omega_{shift}}(t)$, $\omega = 1, 2, 3$, is bigger than the other dimensions at $t = s_\gamma = s_1 = 117.87$, which is x_3 dimension. In Figure 8, the blue curve shows the graph of solution of the system (10), $x_3(t)$, where the initial condition is $x_0 = x(0)$, while the red curve is the solution where the initial value is $x_0 = x(640.35)$, $x_{3_{shift}}(t) = x_3(640.35 + t)$, where $x(t) = (x_1(t), x_2(t), x_3(t))$ and $x_{shift}(t) = (x_{1_{shift}}(t), x_{2_{shift}}(t), x_{3_{shift}}(t))$. The green line segment connects the points $(117.87, x_3(117.87))$ and $(117.87, x_{3_{shift}}(117.87))$.

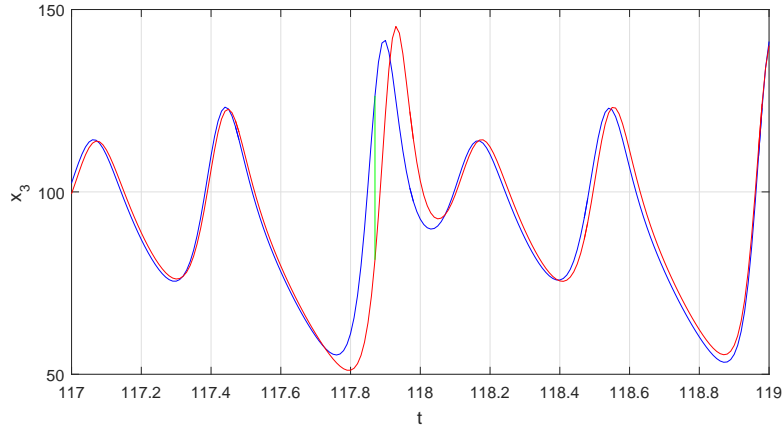


FIGURE 8 The blue curve shows the graph of solution of the system, $x_3(t)$, while the red curve is $x_{3_{shift}}(t)$. The green line segment connects the points $(117.87, x_3(117.87))$ and $(117.87, x_{3_{shift}}(117.87))$ and presents the distance between the solutions at time $t = 117.87$

The length of the green line segment is $|x_3(117.87) - x_{3_{shift}}(117.87)| = 44.93479766$, which is the greatest length between the solution curves until this time in x_3 dimension. In x_1 dimension the greatest length between the solution curves $|x_1(t) - x_{1_{shift}}(t)| = 12.82750911$ occurs at $t = 48.51$, while in x_2 dimension $|x_2(t) - x_{2_{shift}}(t)| = 42.03348827$ occurs at $t = 48.47$. The three-dimensional length at $t = 117.87$ is $\|x(117.87) - x_{shift}(117.87)\| = 47.03608713$, which is the longest until this time value.

If someone proceeds calculating further the distances $\|x(t) - x_{shift}(t)\|$, will notice that all found s_n satisfy the inequality $\|x(s_n) - x_{shift}(s_n)\|$. Going on, we will show that this is true and for others t_n 's. For this purpose we chose four t_k values from Table 3, and in Table 4 we presented the lengths $\|x(t) - x_{shift_l}(t)\|$, where $x_{shift_l}(t) = x(t_l + t)$, for every s_k value of Table 3.

t	$\ x(t) - x_{shift_{t_1}}(t)\ $	$\ x(t) - x_{shift_{t_{79}}}(t)\ $	$\ x(t) - x_{shift_{t_{175}}}(t)\ $	$\ x(t) - x_{shift_{t_{347}}}(t)\ $
$s_1 = 117.87$	47.03608713	47.13469956	47.13803911	47.1349988
$s_{38} = 137.74$	48.96987839	49.09002307	49.09409286	49.0903839
$s_{79} = 160.89$	48.2635579	48.38466658	48.38876917	48.3850257
$s_{111} = 180.69$	46.36700321	46.46176646	46.46497564	46.46204434
$s_{146} = 200.54$	48.85656457	48.96184687	48.96541234	48.96215221
$s_{175} = 217.08$	49.68721677	49.79847211	49.80224005	49.79879175
$s_{207} = 233.63$	48.77836421	48.89884399	48.90292512	48.89918692
$s_{258} = 263.38$	49.70238409	49.81912138	49.82307517	49.81944791
$s_{310} = 293.15$	48.30769663	48.42876336	48.4328644	48.42909614
$s_{347} = 313$	45.86056292	45.98339355	45.98755475	45.98372728

TABLE 4 The distances $\|x(t) - x_{shift_l}(t)\|$ for every s_k value of Table 3, for $l = 1, 79, 175, 347$.

Each of the distances shown above is greater than $\epsilon_0 = 45$, confirming our claim that *every element of the sequence of separations satisfies the inequality $\|x(s_n) - x_{shift_l}(s_n)\| > \epsilon_0$, for every $1 \leq l, n \leq k$* . This result is accurate because of periodicity. Possibly, the sequential test can be applied in this way to recognize or to be at least an additional method for analysis of chaos with multiple periods. Following this result, let us consider the closeness of solutions $x(t)$ and $x_{shift}(t)$ of the system (10) on the interval $[0, 2]$. Figure 9 presents the graph of solutions $x_1(t)$ and $x_{1_{shift}}(t)$ on $[0, 2]$, where the solution curves are near.

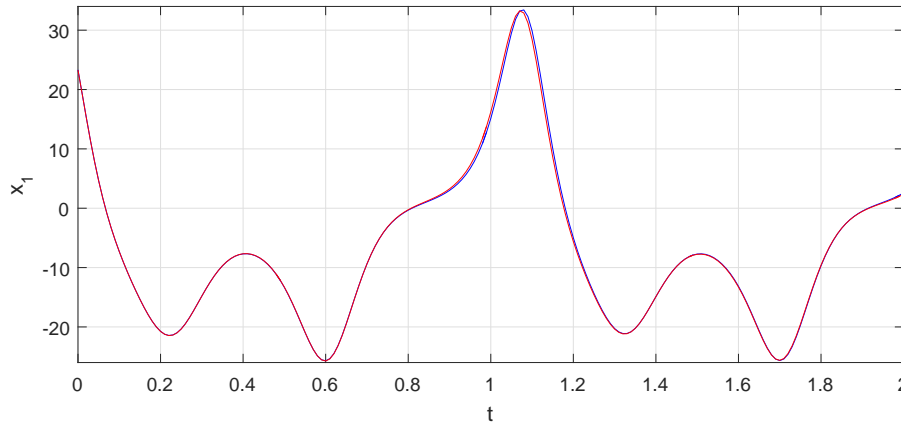


FIGURE 9 The blue and red curve present the solution of $x_1(t)$ and $x_{1_{shift}}(t)$ of system (10) on the interval $[0,2]$. Since these solutions curves are close to each other, in the picture they are seen as a single one (red curve).

One can notice from Figure 9, that the solutions $x_1(t)$ and $x_{1_{shift}}(t)$ are close to each other on the closed intervals $[0,0.82]$, $[1.3,1.57]$, $[1.67,1.71]$ and $[1.81,1.94]$. The greatest distance between the two solution curves on these intervals is 0.092787609. If we consider the three-dimensional graph, the solutions $x(t)$ and $x_{shift}(t)$ are close on the interval $[0.03,0.49]$. From our calculations, the greatest three-dimensional distance between the two solution curves on this interval is 0.096167732.

5 | THE SEQUENTIAL TEST VS. LYAPUNOV EXPONENT CRITERIUM

Many papers were done by applying LEM, to show that a dynamical system is chaotic. The definition of this numerical method is the following.

Definition 9. ⁽²⁾. Let f be a smooth map on \mathbb{R}^m , let $J_n = Df^n(v_0)$, where $Df^n(v_0)$ denote the first derivative matrix of the n th iterate of f , and for $k = 1, 2, \dots, m$, let r_n^k be the length of the k th longest orthogonal axis of the ellipsoid $J_n U$, where U is a unit sphere, for an orbit with initial point v_0 during the first n iterations. The k th **Lyapunov number** of v_0 is defined by

$$L_k = \lim_{n \rightarrow \infty} (r_n^k)^{1/n} \quad (11)$$

if this limit exists. The k th **Lyapunov exponent** of v_0 is $h_k = \ln L_k$. The sequence of iterates $x_0, f(x_0), f^2(x_0) = f(f(x_0)), \dots, f^n(x_0) \dots$ defines an *orbit*.

Following, we apply the sequence test to confirm chaos that has been approved by Lyapunov exponent method.

5.1 | Rössler System

It was firstly introduced by Otto E. Rössler in his paper written on 1976¹⁸. In this paper¹⁸, it was showed that this system is chaotic giving several arguments to show it. The system that we used, which has positive Lyapunov exponents²¹, is the following system:

$$\begin{aligned} x_1' &= -x_2 - x_3 \\ x_2' &= x_1 + 0.2x_2 \\ x_3' &= 0.2 + x_1x_3 - 5.7x_3 \end{aligned} \quad (12)$$

The initial values considered are $[-7.9208550704681606, -0.32213157410506699, 0.01470711076246217]$. Figure 10 (a) shows the trajectory of system (12) having the fixed initial conditions and Figure 10 (b) represents the solution graphs of each coordinate with respect to time t .

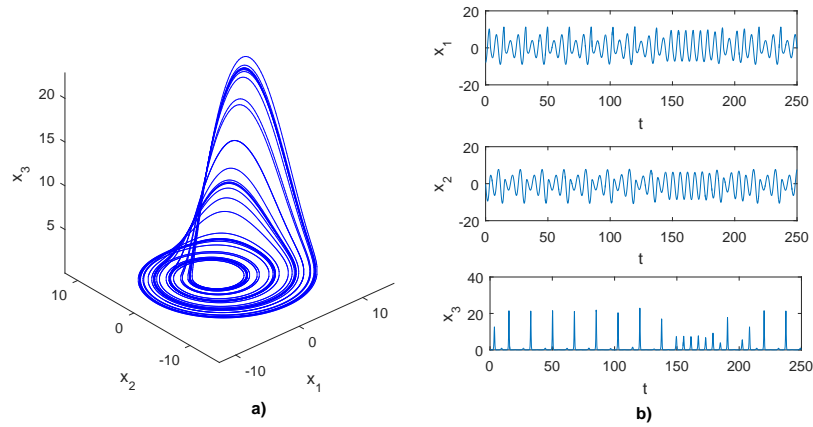


FIGURE 10 Simulations for the solution of system (12) with the given initial values: **(a)** the trajectory of the solution, **(b)** the solution graphs of each coordinate with respect to time t .

We will implement the sequential test through Algorithm 1 to system (12) with the chosen initial condition on interval $[0, 1.9 \cdot 10^6]$ divided into pieces with distance 0.01 and $\varepsilon_0 = 22$. In order that the system (12) satisfy the sequential test for $\varepsilon_0 = 22$, we skipped $t_{fix} = 35$ while finding the sequence of convergence, $\{t_n\}$. For this system we obtained 157 terms for each sequence, and 10 of them are shown in Table 5 .

n	k	$1/k$	t_k	s_k
1	1	1	64.38	20.85
2	16	0.0625	2253.47	512.43
3	30	0.033333	19922.92	916.43
4	56	0.017857	97107.19	2251.43
5	77	0.012987	270473.75	2796.21
6	89	0.011236	405263.82	3024.03
7	111	0.009009	707522.94	3620.64
8	126	0.007937	984335.56	3754.99
9	146	0.006849	1503902.36	3848.64
10	157	0.006369	1878637.91	3848.75

TABLE 5 Selected elements from the sequence of convergence and sequence of separation obtained from Algorithm 1 applied on system (12).

After we acquired the results, let us present the graph of $t_1 = 64.38$, which will be our selected t_γ . Since it is difficult to analyze the three-dimensional graph, we will show graph of solution for system (12) for one dimension with respect to time, the one where the distance between $x_\omega(t)$ and $x_{\omega_{shift}}(t)$, $\omega = 1, 2, 3$, is bigger than the other dimensions at point $t = s_\gamma = s_1 = 20.85$. From our results, the distance at $s_1 = 20.85$ is bigger in x_3 dimension. In Figure 11 , the blue curve shows the graph of solution of (12), $x_3(t)$, where the initial condition is $x_0 = x(0)$, while the red curve is the solution where the initial value is $x_0 = x(64.38)$, $x_{3_{shift}}(t) = x_3(64.38 + t)$, where $x(t) = (x_1(t), x_2(t), x_3(t))$ and $x_{shift}(t) = (x_{1_{shift}}(t), x_{2_{shift}}(t), x_{3_{shift}}(t))$. The green line segment connects the points $(20.85, x_2(20.85))$ and $(20.85, x_{2_{shift}}(20.85))$.

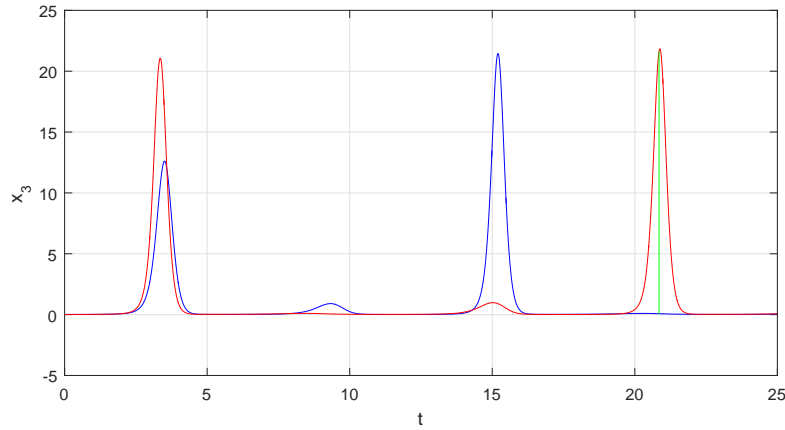


FIGURE 11 The blue curve shows the graph of solution of the system, $x_3(t)$, while the red curve is $x_{3_{shift}}(t)$. The green line segment connects the points $(20.85, x_2(20.85))$ and $(20.85, x_{2_{shift}}(20.85))$ and presents the distance between the solutions at time $t = 20.85$

If someone would calculate the distance of the green segment would have found that $|x_3(20.85) - x_{3_{shift}}(20.85)| = 21.57182863$, which is the greatest length between the solution curves until this time in x_3 dimension. In x_1 dimension the greatest length between the solution curves $|x_1(t) - x_{1_{shift}}(t)| = 7.887399774$ occurs at $t = 20.46$, while in x_2 dimension $|x_2(t) - x_{2_{shift}}(t)| = 8.506374252$ occurs at $t = 19.49$. The three-dimensional length at $t = 20.85$ is $\|x(20.85) - x_{shift}(20.85)\| = 22.08237084$, which is the largest until this time value.

Following this result, let us consider the closeness of solutions $x(t)$ and $x_{shift}(t)$ of the system 12 on the interval $[822, 870]$. Figure 12 presents the graph of solutions $x_3(t)$ and $x_{3_{shift}}(t)$ on $[822, 870]$, where the solution curves are imminent.

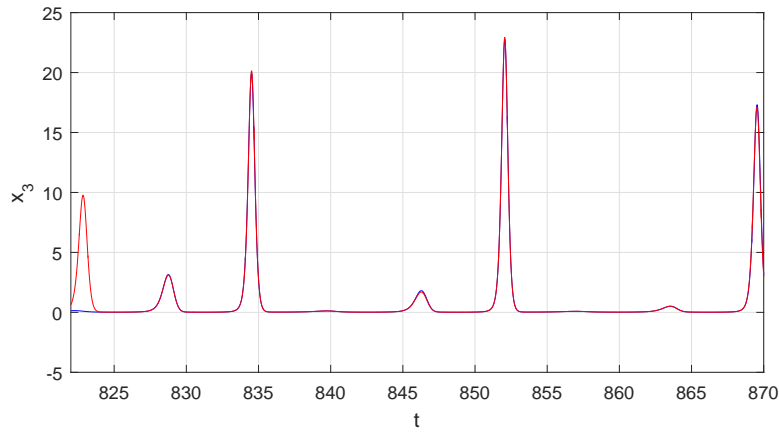


FIGURE 12 The blue and red curve present the solution of $x_3(t)$ and $x_{3_{shift}}(t)$ of system (12) on the interval $[822, 870]$.

It is seen from Figure 12, that the solutions $x_3(t)$ and $x_{3_{shift}}(t)$ are close to each other on the closed interval $[823.79, 869.51]$. The greatest distance between the two solution curves on this interval is 0.099134999. If we consider the three-dimensional graph, the solutions $x(t)$ and $x_{shift}(t)$ are close on the closed interval $[823.8, 865.06]$. The greatest three-dimensional distance between the two solution curves on this interval is 0.099931352.

5.2 | Ikeda Map

In this subsection, we considered the following equation taken from the book², where it was proven that equation (13) has positive Lyapunov exponents.

$$\begin{aligned} x_{n+1} &= 1 + 0.9(x_n \cos(\tau_n) - y_n \sin(\tau_n)) \\ y_{n+1} &= 0.9(x_n \sin(\tau_n) + y_n \cos(\tau_n)) \end{aligned} \quad (13)$$

where $\tau_n = 0.4 - (\frac{6}{1+x_n^2+y_n^2})$

For this system we took as initial conditions $[0, 0]$. Figure 13 (a) shows the trajectory of system (13) within initial conditions and Figure 13 (b) represents the solution graphs of each coordinate with respect to index i .

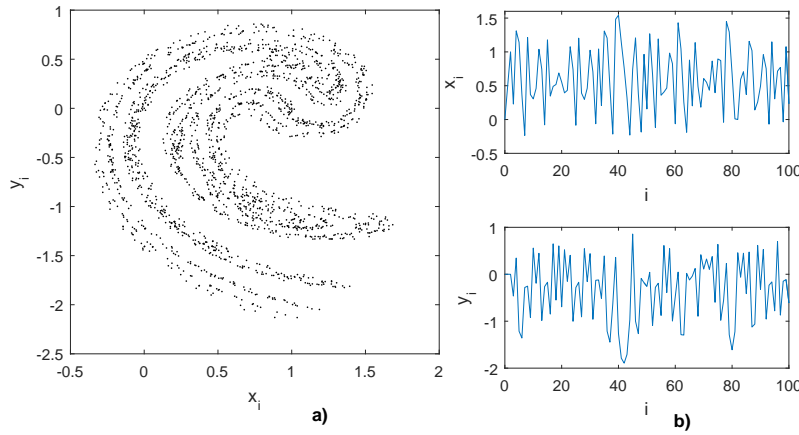


FIGURE 13 Simulations for the solution of system (13) with the given initial values: **(a)** the trajectory of the solution, **(b)** the solution graphs of each coordinate with respect to index i .

We will perform the sequential test through Algorithm 2 to system (13) with the chosen initial condition and $\varepsilon_0 = 2$. Index interval starts from 0 and prolongs till $3 * 10^6$. As a result, we obtained 754 terms for each sequence, and selected 11 of them are shown in Table 6 .

n	k	$1/k$	t_k	s_k
1	1	1	2	34
2	16	0.0625	1193	384
3	95	0.010526	204042	1175
4	160	0.00625	1236723	2221
5	201	0.004975	2394484	2920
6	289	0.00346	8255283	4048
7	354	0.002825	14874258	4947
8	407	0.002457	22484165	5858
9	520	0.001923	51130431	7508
10	693	0.001443	161661433	9873
11	754	0.001326	295347460	10735

TABLE 6 Selected elements from the sequence of convergence and the sequence of separation obtained from Algorithm 2 applied on system (13).

After we acquired the results, let us sketch the graph for one of them, say the graph associated with $\zeta_\gamma = \zeta_{16} = 1193$. Since it is difficult to analyze the two-dimensional graph, we will show the graph of system (13) for one dimension, the one where the distance between $\omega_i = \omega(i)$ and $\omega_{shift}(i)$, $\omega = x, y$, is bigger than the other dimensions at index $i = \eta_\gamma = \eta_{16} = 384$. The distance at $\eta_{16} = 384$ is bigger in y dimension. In Figure 14, the blue curve shows the graph of solution of (13), $y_i = y(i)$, where the initial condition is $X_0 = X(0)$, while the red curve is the solution where the initial value is $X_0 = X(1193)$, $y_{shift}(i) = y(1193+i)$, where $X(i) = (x(i), y(i))$ and $X_{shift}(i) = (x_{shift}(i), y_{shift}(i))$. The green line segment connects the points $(384, y(384))$ and $(384, y_{shift}(384))$.

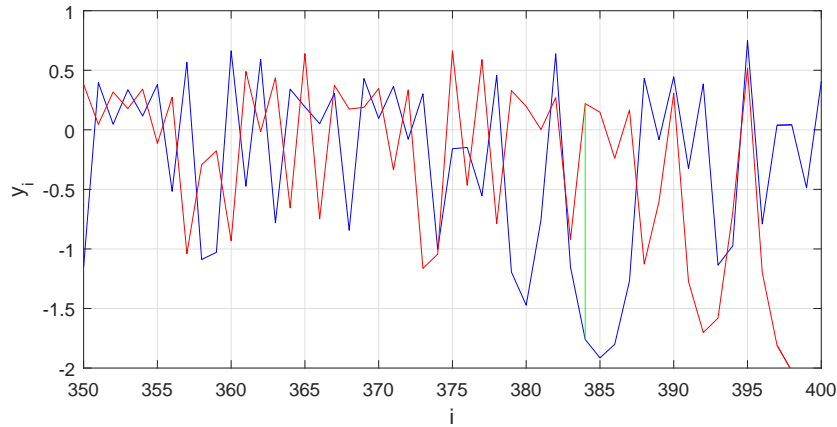


FIGURE 14 The graph for system (13) with respect to y_i and index i . The blue line shows the graph of solution of the system, $y(i)$, while the red line is $y_{shift}(i)$. The green line segment connects the points $(384, y(384))$ and $(384, y_{shift}(384))$ and presents the distance between the solutions at index $i = 384$

From our calculations, we can noticed that the length of the green segment $|y(384) - y_{shift}(384)| = 1.980393236 < \epsilon_0$ is not the greatest until the index $i = 384$. Someone can find that

$$\begin{aligned} |y(22) - y_{shift}(22)| &= 2.350274265, \\ |y(38) - y_{shift}(38)| &= 2.085833749, \\ |y(40) - y_{shift}(40)| &= 2.261857315, \\ |y(42) - y_{shift}(42)| &= 2.175361502, \\ |y(55) - y_{shift}(55)| &= 2.143415044, \\ |y(95) - y_{shift}(95)| &= 1.983853779, \\ |y(106) - y_{shift}(106)| &= 2.239737095, \\ |y(128) - y_{shift}(128)| &= 1.991610248, \\ |y(129) - y_{shift}(129)| &= 2.243506045, \\ |y(131) - y_{shift}(131)| &= 2.434072116, \\ |y(190) - y_{shift}(190)| &= 2.145400124, \\ |y(192) - y_{shift}(192)| &= 2.212754503, \\ |y(212) - y_{shift}(212)| &= 2.348997502, \\ |y(239) - y_{shift}(239)| &= 2.014821546, \\ |y(242) - y_{shift}(242)| &= 2.167259729, \\ |y(282) - y_{shift}(282)| &= 2.281796984, \\ |y(288) - y_{shift}(288)| &= 2.500601744. \end{aligned}$$

Investigating these results, except the distance at $i = 95$, all other distances are bigger than ϵ_0 . Except for these indexes, this is also evident at two-dimensional distances

$$\begin{aligned} \|X(20) - X_{shift}(20)\| &= 2.112599494, \\ \|X(95) - X_{shift}(95)\| &= 2.007853134, \end{aligned}$$

$$\begin{aligned}
\|X(120) - X_{shift}(120)\| &= 2.012945907, \\
\|X(123) - X_{shift}(123)\| &= 2.211804315, \\
\|X(125) - X_{shift}(125)\| &= 2.147501466, \\
\|X(126) - X_{shift}(126)\| &= 2.219332021, \\
\|X(184) - X_{shift}(184)\| &= 2.033164228, \\
\|X(189) - X_{shift}(189)\| &= 2.084321694, \\
\|X(239) - X_{shift}(239)\| &= 2.015012267, \\
\|X(244) - X_{shift}(244)\| &= 2.304006889, \\
\|X(284) - X_{shift}(284)\| &= 2.151226213, \\
\|X(285) - X_{shift}(285)\| &= 2.025867605,
\end{aligned}$$

The distance for both dimensions at $i = 384$ is $\|X(384) - X_{shift}(384)\| = 2.293721422$. Next, let us consider the closeness of solutions $X(i)$ and $X_{shift}(i)$ of the system (13) on the interval $[2600, 2650]$. Figure 15 presents the graph of solutions $y(i)$ and $y_{shift}(i)$ on $[2600, 2650]$, where the solution curves are nigh.

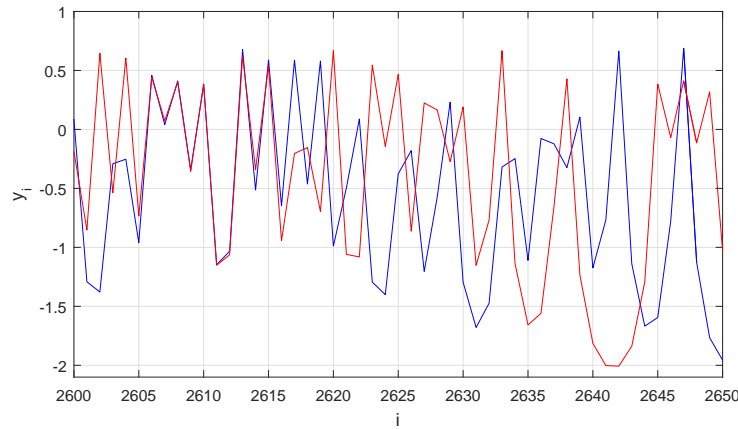


FIGURE 15 The blue and red curve present the solution of $y(i)$ and $y_{shift}(i)$ of system (13) on the interval $[2600, 2650]$.

From Figure 15, one can notice that the solutions $y(i)$ and $y_{shift}(i)$ are close to each other on the closed interval $[2606, 2615]$. The greatest distance between the two solution curves on this interval is 0.054321108. If we consider the two-dimensional graph, the solutions $X(i)$ and $X_{shift}(i)$ are close on the closed interval $[2607, 2612]$. The greatest two-dimensional distance between the two solution curves on this interval is 0.041486722.

5.3 | Intermittency

Intermittency or intermittent chaos is a periodic motion where at some specific time chaotic motions burst¹¹. The most well-known intermittent system¹, which has positive Lyapunov exponents, is:

$$\begin{aligned}
x'_1 &= 10(x_2 - x_1) \\
x'_2 &= -x_1x_3 + 166.29x_1 - x_2 \\
x'_3 &= x_1x_2 - \frac{8}{3}x_3
\end{aligned} \tag{14}$$

Let the initial conditions be $[-6.9027101537827207, 6.1214285868616205, 146.73481404307805]$. Figure 16 (a) shows the trajectory of system (14) having the fixed initial conditions, while Figure 16 (b) represents the solution graphs of each coordinate with respect to time t .

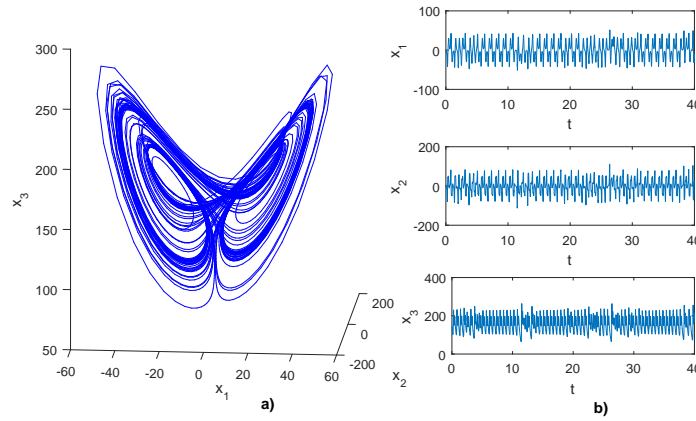


FIGURE 16 Simulations for the solution of system (14) with the given initial values: **(a)** the trajectory of the solution, **(b)** the solution graphs of each coordinate with respect to time t .

We will apply Algorithm 1 on system (14) with the chosen initial condition and $\varepsilon_0 = 200$. Time interval starts from 0 and prolongs till $1.5 \cdot 10^6$, partitioned into pieces with distance 0.01. In order that the system (14) satisfy the sequential test for $\varepsilon_0 = 200$, we skip $t_{fix} = 11.64$ while finding the sequence $\{t_n\}$. Within the given conditions and time interval, we found that $k = 91$. In Table 7, are shown 10 selected elements from the sequence of convergence and the sequence of separation.

n	k	$1/k$	t_k	s_k
1	1	1	15.43	96.98
2	12	0.083333	2994.48	2322.64
3	23	0.043478	12029.93	4237.28
4	31	0.032258	51983.29	6852.58
5	45	0.022222	162216.36	11141.28
6	56	0.017857	401509.63	14399.56
7	63	0.015873	580535.22	16311.43
8	70	0.014286	802996.63	18649.65
9	79	0.012658	1016186.84	20581.15
10	91	0.010989	1420323.21	24758.91

TABLE 7 Selected elements from the sequence of convergence and the sequence of separation obtained from Algorithm 1 applied on system(14).

Succeeding, we will sketch the graph of one element of the sequence of convergence exhibited in Table 7, say for $t_\gamma = t_1 = 15.43$. Since it is difficult to analyze the three-dimensional graph, we will show graph of solution for system (14) for one dimension with respect to time, the one where the distance between $x_\omega(t)$ and $x_{\omega_{shift}}(t)$, $\omega = 1, 2, 3$, is bigger than the other dimensions at time $t = s_\gamma = s_1 = 96.98$, which occurs in x_2 dimension. In Figure 17, the blue curve shows the graph of solution of (14), $x_2(t)$, where the initial condition is $x_0 = x(0)$, while the red curve is the solution where the initial value is $x_0 = x(15.14)$, $x_{2_{shift}}(t) = x_2(15.43 + t)$, where $x(t) = (x_1(t), x_2(t), x_3(t))$ and $x_{shift}(t) = (x_{1_{shift}}(t), x_{2_{shift}}(t), x_{3_{shift}}(t))$. The green line segment connects the points $(96.98, x_2(96.98))$ and $(96.98, x_{2_{shift}}(96.98))$.

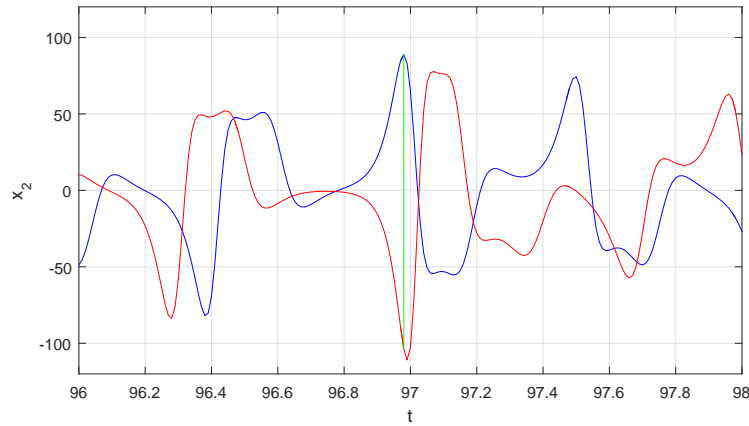


FIGURE 17 The blue curve shows the graph of solution of system (14), $x_2(t)$, while the red curve is $x_{2_{shift}}(t)$. The green line segment connects the points $(96.98, x_2(96.98))$ and $(96.98, x_{2_{shift}}(96.98))$ and presents the distance between the solutions at time $t = 96.98$

The length of the green line segment is $|x_2(96.98) - x_{2_{shift}}(96.98)| = 192.44361$, which is the greatest length between the solution curves until this time in x_2 dimension. In x_1 dimension the greatest length between the solution curves $|x_1(t) - x_{1_{shift}}(t)| = 84.04897$ occurs at $t = 25.1$, while in x_3 dimension $|x_3(t) - x_{3_{shift}}(t)| = 173.93722$ occurs at $t = 47.51$. The three-dimensional distance at $t = 96.98$ is $\|x(96.98) - x_{shift}(96.98)\| = 207.9604947$, which is the biggest until this point.

Following this result, let us consider the closeness of solutions $x(t)$ and $x_{shift}(t)$ of the system (14) on the interval $[4772, 4786]$. Figure 18 presents the graph of solutions $x_2(t)$ and $x_{2_{shift}}(t)$ on $[4772, 4786]$, where the solution curves are near.

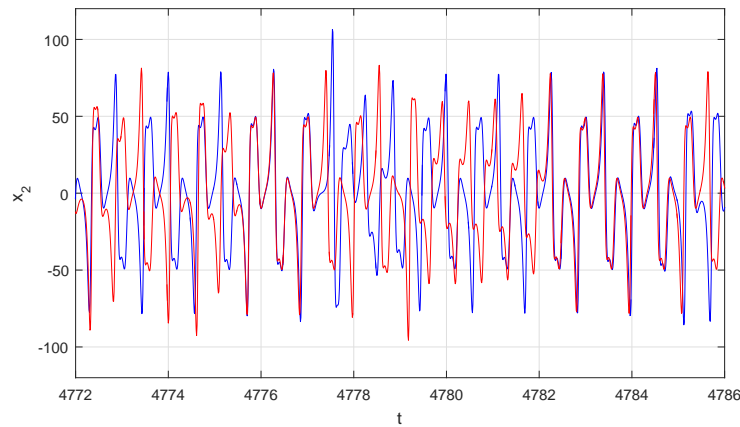


FIGURE 18 The blue and red curve present the solution of $x_2(t)$ and $x_{2_{shift}}(t)$ of system (14) on the interval $[4772, 4786]$.

It is seen from Figure 18, that the solutions $x_2(t)$ and $x_{2_{shift}}(t)$ are close to each other on the closed intervals $[4775.88, 4776.07]$ and $[4776.53, 4776.56]$. The greatest distance between the two solution curves on these intervals is 0.469810895. If we consider the three-dimensional graph, the solutions $x(t)$ and $x_{shift}(t)$ are close on the closed interval $[4775.88, 4776.07]$. The greatest three-dimensional distance between the two solution curves on this interval is 0.527310061.

References

1. Y. AIZAWA, Symbolic Dynamics Approach to Intermittent Chaos, *Progress of Theoretical Physics* **70** (1983), 1249–1263.
2. K. T. ALLIGOOD, T. D. SAUER, J. A. YORKE, *CHAOS: An Introduction to Dynamical Systems*, Springer, United States of America, 1996.
3. M. U. AKHMET, M. O. FEN, Replication of chaos, *Commun. Nonlinear Sci. Numer. Simul.* **18** (2013), 2626–2666.
4. M. U. AKHMET, M. O. FEN, *Replication of Chaos in Neural Networks, Economics and Physics*, Springer & HEP, Berlin, Heidelberg, 2016.
5. M. AKHMET, M. O. FEN, Poincaré chaos and unpredictable functions, *Commun. Nonlinear Sci. Numer. Simulat.* **48** (2017), 85–94.
6. M. AKHMET, M. O. FEN, Unpredictable points and chaos, *Commun. Nonlinear Sci. Numer. Simulat.* **40** (2016), 1–5.
7. M. AKHMET, M. O. FEN, Non-autonomous equations with unpredictable solutions, *Commun. Nonlinear Sci. Numer. Simulat.* **59** (2018), 657–670.
8. D. V. ANOSOV, Geodesic flows and closed Riemannian manifolds with negative curvature, *Proc. Steklov Inst. Math.* **90** (1967).
9. R. DEVANEY, *An Introduction to Chaotic Dynamical Systems*, Addison-Wesley, United States of America, 1987.
10. S. M. HAMMEL, J. A. YORKE, C. GREBOKI, Do numerical orbits of chaotic dynamical processes represent true orbits?, *J. Complex* **3** (1987), 136–145.
11. T. KOHYAMA, Y. AIZAWA, Theory of the Intermittent Chaos, *Progress of Theoretical Physics* **71** (1984), 917–929.
12. T. Y. LI, J. A. YORKE, Period three implies chaos, *The American Mathematical Monthly* **82** (1975), 985–992.
13. E. N. LORENZ, Deterministic non-periodic flows, *Journal of the Atmospheric Science* **20**(1963), 130–141.
14. K. PALMER, *Shadowing in Dynamical Systems: Theory and Applications*, Kluwer Academic Publishers, Dordrecht, 2000.
15. S. Y. PILUGIN, *Shadowing in Dynamical Systems*, Springer, Berlin, 1999.
16. C. ROBINSON, *An Introduction to Dynamical Systems: Continuous and Discrete*, Pearson, United States of America, 2004.
17. C. ROBINSON, *Dynamical Systems: Stability, Symbolic Dynamics, and Chaos*, CRC Press, Boca Raton, 1995.
18. O. E. RÖSSLER, An equation for continuous chaos, *Physics Letters.* **57A** (1976), 397–398
19. SELL, G. R., *Topological Dynamics and Ordinary Differential Equations*, Van Nostrand Reinhold Company, London, 1971.
20. Y. UEDA, R. ABRAHAM, *The Chaos Avant-Garde: Memories of the early days of chaos theory*, World Scientific Publishing, Singapore, 2000.
21. J. C. SPROTT, ASYMMETRIC BISTABILITY IN THE RÖSSLER SYSTEM, *Acta Physica Polonica B* **48** (2017), 97–107.

